UNDERSTANDING WIND-GENERATED INFRASOUND NOISE

Robert Woodward[1], Hans Israelsson[1], István Bondár[1],
Keith McLaughlin[1], J. Roger Bowman[1], and Henry Bass[2]

Science Applications International Corporation[1]
National Center for Physical Acoustics, University of Mississippi[2]

Sponsored by Army Space and Missile Defense Command

Contract Nos. DASG60-03-C-0009[1] and DASG60-99-C-0018[2]

ABSTRACT

We have analyzed wind-generated pressure noise at infrasound stations to better understand the mechanisms of noise generation and possible strategies for mitigating the effects of this noise. Wind and microbaroms are the dominant sources of noise on infrasound stations. Both can cause false signal detections as well as obscure real signals. We have investigated in detail the observed wind and pressure characteristics at International Monitoring System infrasound stations. By understanding better the relationship of wind and pressure, we can design signal detection algorithms which mitigate the impact of wind-generated noise.

We analyzed variations in wind speed and pressure noise over long periods of time (up to two years). The goal of this analysis is to better understand seasonal, diurnal, or other variations in these quantities so that we may better understand their relationship. We see that the ambient pressure noise is highly variable by season, time of day, station and site type. The pressure noise is correlated to horizontal wind speed above a threshold value, and this threshold varies by station and is often between 0.5-1.5 m/s.

We have computed pressure spectra for time periods with different average wind speeds and see relatively consistent spectra, particularly when these spectra are displayed as a function of frequency normalized by wind speed. Wind speed spectra calculated for time periods of relatively high wind speeds often have slopes around -5/3, a characteristic of so called Kolmogorov turbulence. Wind turbulence can vary substantially at the stations, with periods of low winds often having the highest turbulence. Individual stations show substantial variations in wind turbulence as a function of wind direction, which may be related to the terrain and vegetation at the infrasound station.

We have considered two primary approaches to characterizing the relationship between wind and pressure variations. First, we develop an empirical model for pressure noise as a function of wind speed. We find a clear relationship between wind speed and pressure, which varies by station and frequency band. The empirical model is characterized by the slope of the pressure-wind relationship and shows a clear distinction (change in slope) between low- and high-wind regimes, though the wind speed at which this change occurs varies by station. We assess the ability of this model to predict root-mean-square (RMS) pressure variations based on observations of wind. For test cases the standard error of predictions was 3db or less for frequency bands above 0.5 Hz and wind speeds above 1.5 m/s. A key variable is the time varying nature of the empirical model. We also seek to understand how long it takes to characterize the wind speed-to-pressure relationship and to determine how frequently it must be updated.

We have used a statistical framework for our second approach to characterizing the wind speed-pressure relationship. We analyze extreme values of wind and noise (i.e. the tails of the distributions of these observations) via copula functions. The copula function analysis lets us characterize the joint probability distribution of wind and pressure variations. By understanding this relationship, we can estimate the probability that large values of pressure are due to wind. This relationship can ultimately be used to design signal detectors with a constant false alarm rate (for wind-induced false alarms) by dynamically adjusting detection thresholds based on wind speed.

OBJECTIVES

Our objective has been to improve our understanding of the underlying physical processes responsible for noise at infrasound stations, particularly wind-generated noise. We then leverage this understanding to develop noise mitigation strategies.

RESEARCH ACCOMPLISHED

Data

We have used data from virtually all current infrasound stations (Figure 1). All of these stations are arrays consisting of 4 to 9 elements. Twenty-nine stations are part of the International Monitoring System (IMS) network, and five are experimental stations. The stations contain different combinations of microbarometer, digitizer, and wind filter design, as well as different array geometries. Data are obtained from the data archive operated by the Research and Development Support Services (RDSS) project of the US Army Space and Missile Defense Command's Monitoring Research Program (MRP)

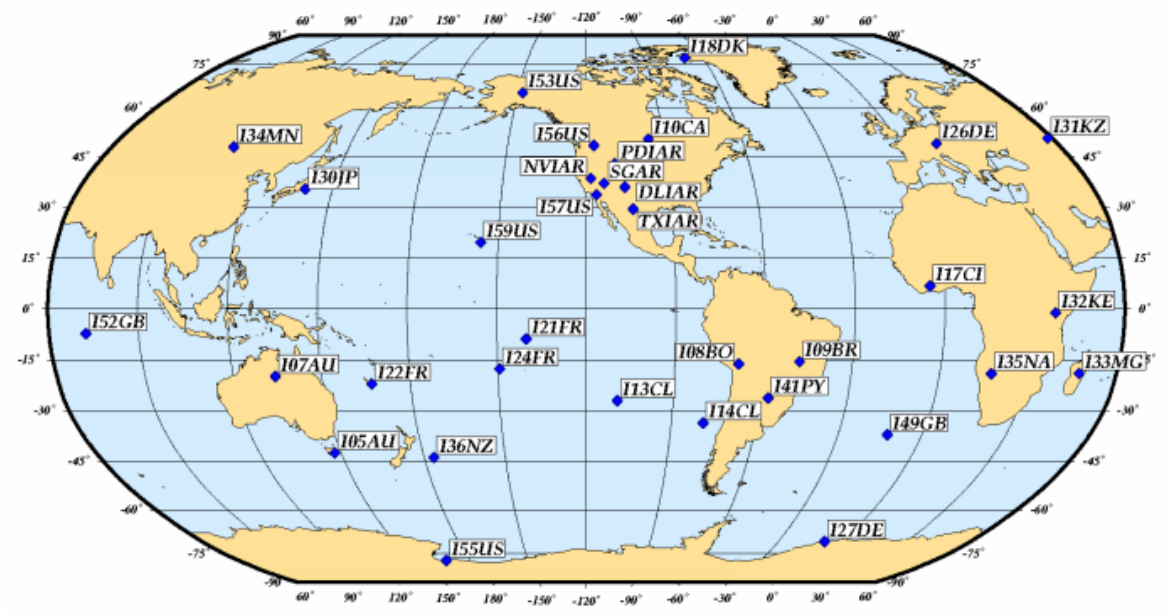

Figure 1. Map showing a superset of the infrasound stations used in our analyses.

Infrasound Noise

In order to characterize the ambient noise, power spectral density was measured at 28 stations (Figure 1) using the approach of Bowman et al. (2004a, b, 2005a, b). Data were analyzed from January 20, 2003 through December 31, 2004, from 21 consecutive 3-minute segments of data taken four times daily, beginning at 06:00, 12:00, 18:00, and 24:00 local time, resulting in 1,476,309 spectral estimates. Three-minute windows were used to minimize smoothing of the amplitude distributions, while permitting estimation of the longest periods of interest. Spectra were calculated using *geotool* (Coyne and Henson, 1995) and the method of overlapping fast Fourier transforms. A Hanning taper was applied to the outer 10% of each data window. Spectra were corrected by *geotool* for instrument responses in the RDSS data archive database.

Power Spectral Density (PSD) for noise in four seasons and at four times of day are shown in Figure 2 for station I57US at Piñon Flat, California. All spectra calculated for each time and season interval are plotted as yellow lines, the median for each interval as a black line, and the 5th and 95th percentiles of the distribution as red lines. Green lines show the median of all spectra for all times and seasons for 15 stations having a complete year of data, and thus serve as references for comparison among time and season intervals and among stations. At any time, season and frequency the PSD varies by four to five orders of magnitude. Seasonal and diurnal variations are evident among the subplots. For example, the median noise level is similar to the network median at 6 AM in spring, but is almost an

order of magnitude lower at the same time in summer, and is an order of magnitude higher in the same season at noon. Plots similar to those in Figure 2 are provided for nearly all current infrasound stations (28 in all) in Bowman et al. (2005b).

Relationship of Micropressure and Wind

It is well known that infrasound noise increases as wind speed near the sensor increases. For example, Figure 3 illustrates wind-induced noise due to diurnal variations at I08BO, Bolivia. The large amplitudes on the micropressure channels due to wind can cause false signal detections. Conversely, the wind-generated noise can reduce signal coherence across the array and result in no detections at all, particularly for detection algorithms which exploit the across-array coherence of signals.

We have characterized the gross relationship between noise and horizontal wind speed at all stations having wind speed data. Wind speeds are calculated for the same time intervals used for the ambient noise analysis reported above (Bowman, 2005a, b). This provides nearly a million simultaneous micropressure and wind speed observations.

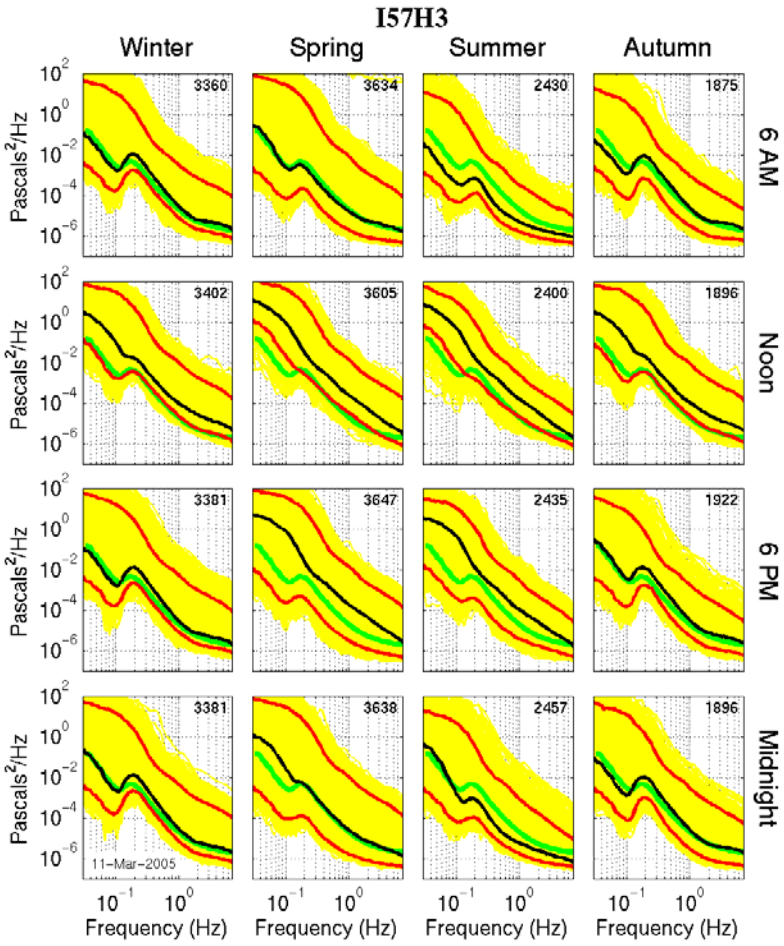

Figure 2. Power Spectral Density for I57US (I57US), Piñon Flat, California. The number of spectra in each plot is shown in the upper right. The rows group plots by time intervals, the columns group plots by seasons.

Figure 4 shows a comparison of noise at 0.2 Hz versus wind speed for several stations. Similar plots for a larger set of 22 stations which have wind speed data are provided in Bowman et al. (2005b). Examining the noise versus wind speed observations for all 22 stations indicates there is wide variability in the range of wind speeds and the range of associated micropressure fluctuations. The most basic observation from this analysis is that noise at most stations

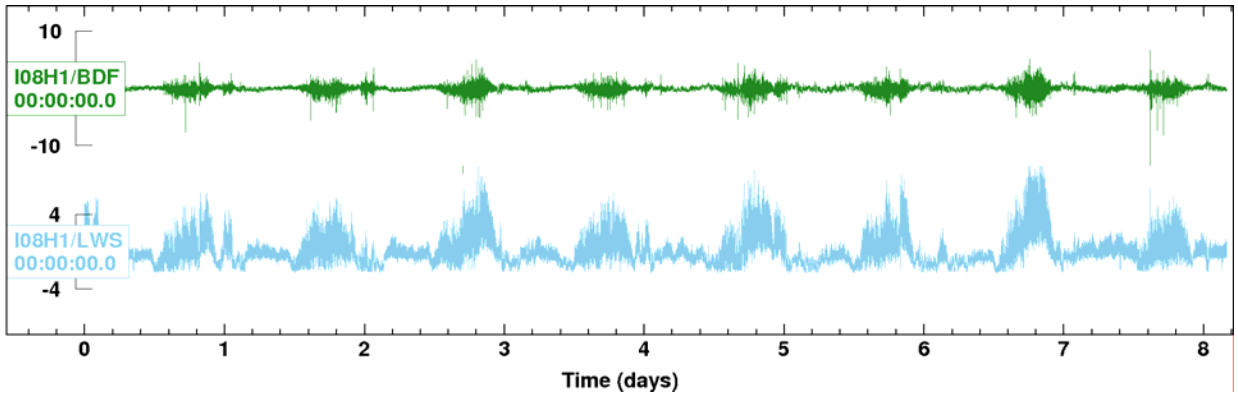

Figure 3. Micropressure data (top trace) and wind speed (bottom trace) at I08BO between May 1 and 8, 2005. Note how the micropressure noise levels increase with increasing wind speed.

increases gradually up to some wind threshold, and then increases more rapidly at higher wind speeds. Note that at stations I55US (shown in Figure 4) and I27DE (not shown) in Antarctica this wind threshold is at a higher value, possibly due to the fact that the wind filters at these stations are buried in snow at least part of the year. The relationship between infrasound noise at 1 Hz and wind speed is similar to that at 0.2 Hz (Bowman et al., 2005b).

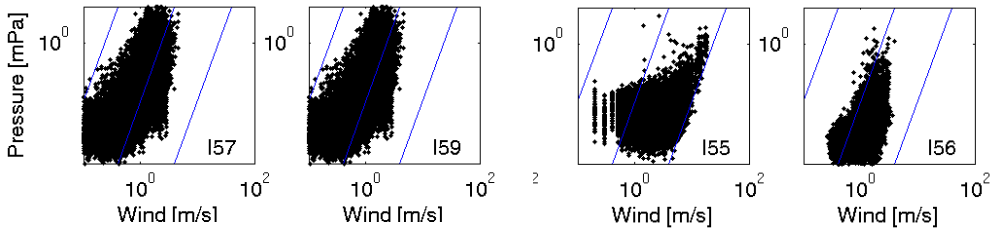

Figure 4. Relationship between ambient infrasound noise at 0.2 Hz and horizontal wind speed, on log-log scales. The blue reference lines are spaced in decade intervals in wind speed and aid in comparison among plots. Vertical groupings of data points for I55 are the result of truncation of wind speed to integer values (in m/s) for part of the observation period.

Wind and Micropressure Power Spectra

We have investigated the micropressure and wind speed power spectra in greater detail using a representative subset of IMS stations: I08BO, I17CI, I18DK, I22FR, I24FR, I31KZ, I33MG, I34MN, and I35NA (Israelsson and McLaughlin, 2005). For these analyses we used a data window of 3 min. for consistency with ambient noise spectral calculations reported above (Bowman et al., 2005a).

Figure 5 (top) shows averaged wind speed spectra at I08BO at wind speeds between 3-7 m/s. The drop off rate of the scaled spectra for I08BO have a slope of approximately -5/3 (heavy dashed lines in the diagrams) predicted for Kolmogorov turbulence of the inertial regime. Further, the spectra for different wind speeds, when scaled by wave-number (frequency/wind speed), collapse into a narrow spectral density range (Figure 5, bottom). Similar results were obtained for stations I24FR and I35NA, while the slopes of spectra for I31KZ and I34MN clearly deviated from -5/3 throughout the wave-number range. The wave-number intervals with slopes ~ -5/3 correspond to wavelengths between 10-100 m.

The IMS stations analyzed here are equipped with two types of wind sensors, cup anemometers (Campbell) and ultrasonic sensors (Gill). The overall shape of average wind spectra at the five stations with cup anemometers are similar, whereas there is more variation in shapes among average spectra at the four stations using ultrasonic sensors. The power spectra for stations with cup instruments tend to flatten out at high frequencies for low wind speeds less than about 2 m/s, which might be caused by inertia of the instruments.

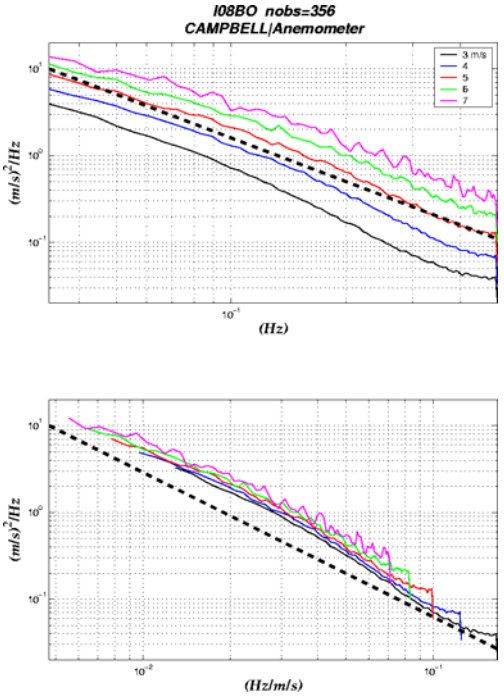

Figure 5. Comparison of power spectra for wind speed fluctuations at different wind speeds (3-7 m/s) at station I08BO as a function of frequency (top) and as a function of wave-number (bottom). The heavy dashed lines have a slope of -5/3

Power spectra of micropressure are binned by mean wind speed, followed by stacking of spectra in each bin on a daily basis. The stacking reduces the scatter in the data and was motivated by the pronounced diurnal variation of the wind speed at most of the stations. Figure 6 shows averaged micropressure power spectra, as a function of frequency (top) and as a function of frequency/wind speed, (bottom), for wind speeds between 3 to7 m/s. The dashed lines in the lower panel of Figure 6 has a slope of -7/3, which is expected in the inertial range of turbulence from dimensional analysis, although this drop off in power with wave-number is not generally agreed upon (Shields, 2005). When plotted as a function of wave-number the spectra lie closer together at low wave-numbers between about 0.01-0.04 m^{-1}, where the spectra drop off with a slope of approximately -7/3. Similar results were obtained for I18DK, I34MN, and I35NA. Wave-numbers between 0.01 and 0.04 m^{-1} correspond to wavelengths between 25-100 m, in which range wind spectra for I08BO drop off with a slope around -5/3. This suggests that the I08BO spectra at low wave-numbers, for both wind and micropressure, are in qualitative agreement with standard models for the inertial subrange of turbulence for the two stations.

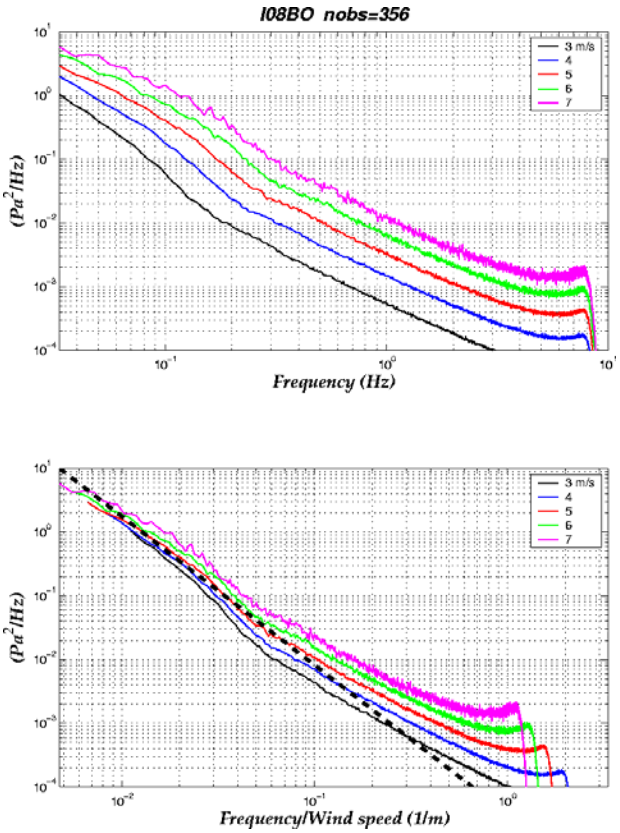

Figure 6. Comparison of power spectra for micropressure for different wind speeds (3-7 m/s) at station I08BO as a function of frequency (top) and as a function of wave-number (bottom). The heavy dashed line is provided for reference and has a slope of -7/3.

Prediction Using Empirical Relationship of Micropressure and Wind

As noted earlier, sudden large amplitudes on micropressure recordings can be due to signals or noise from wind gusts. In this section we attempt to exploit the high correlation between micropressure and wind speed to predict micropressure amplitudes from wind speed. Such predictions would allow us to identify features in the micropressure record that are explained by wind (potential false alarms) and features that cannot be explained by the wind (potential signals).

For these predictions we calculated RMS amplitudes of micropressure recordings in six non-overlapping one octave frequency bands (0.01-0.05, 0.05-0.10, 0.10-0.5, 0.5-1.0, 1-2, and 2-4 Hz) using a data window of 600 s with a 50% overlap between consecutive windows. In addition, the mean wind speed and its NS and EW components were calculated along with the RMS of the wind speed fluctuations for the same data windows. Figure 7 shows the logarithm of RMS micropressure as a function of the logarithm of average wind speed, for station I08BO. The logarithmic transformation enhances resolution at low wind speeds. We use locally robust regression to estimate the relationship between RMS micropressure and wind, and this is shown by the dashed line in Figure 7.

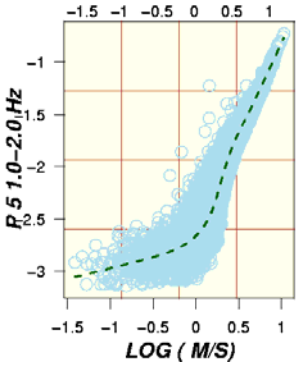

Figure 7. RMS micropressure (1-2 Hz band) as a function of average wind speed at I08BO. The data points represent the logarithms of RMS micropressure and wind measurements.

A comparison of the estimated RMS (1-2 Hz) micropressure and mean wind speed relationships for nine different stations are shown in Figure 8. The estimates have similar slopes at high wind speeds, and large variation at low wind speeds where the levels are affected by the microbarom levels.

In prediction experiments we used data for the first half of the month to estimate relations between micropressure and wind. The estimates were then used to predict RMS micropressure amplitudes during the second half of the month. Figure 9 shows an example of time domain micropressure predictions. Predicted RMS amplitudes in the frequency band 1-2 Hz at I08BO during the second half of October 2004 are compared with the actual amplitudes and the mean wind speed. The predictions were based on a relation between RMS amplitudes and mean wind speed estimated with locally robust regression from observations during the first half of October 2004. The traces for mean wind speed, observed and predicted RMS amplitudes (three bottom traces) are quite similar with a clear diurnal variation. The ratio of the predicted-to-observed pressures (in dB) is plotted in the top trace and the difference (predicted – observed) in the trace below. The ±3dB error levels are marked as dashed lines on the top trace. The errors, just like the wind speed and RMS amplitudes, show a diurnal variation. The relative errors (see top trace) are generally larger during periods of low wind speeds during local night time than during local day time with high wind speeds. The magnitude of the errors (e.g. second trace from top) is greatest in the day time.

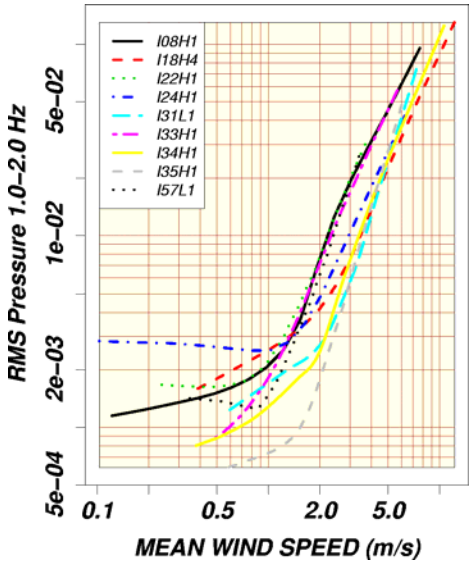

Figure 8. Estimated relations between RMS micropressure (1-2 Hz) and mean wind speed for October 2004.

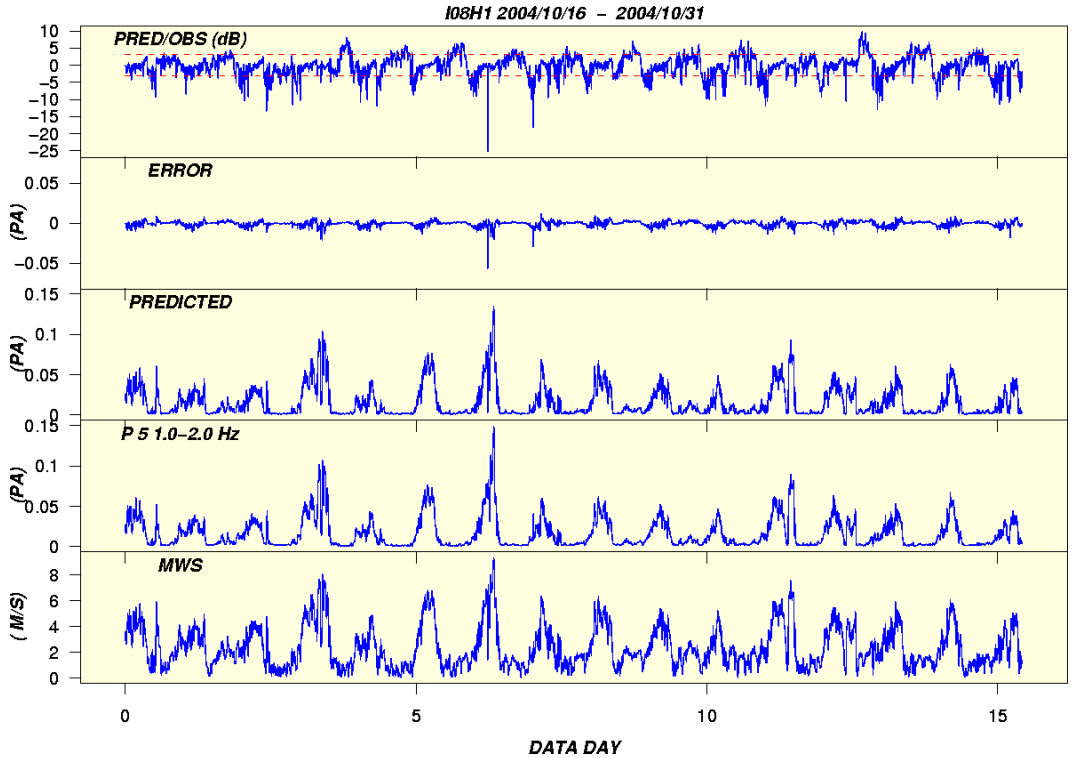

Figure 9. Comparison of observed and predicted RMS amplitudes (1-2 Hz) at I08BO during Oct 16-31, 2004. The traces for mean wind speed (bottom trace), observed RMS amplitudes (2nd trace from bottom), and predicted amplitudes (3rd trace from bottom) are quite similar. A clear diurnal variation is obvious in the ratios of predicted/observed amplitudes (top trace) and amplitudes errors, observed-predicted, (2nd trace from top).

The dependence of prediction error on wind speed indicates that the estimated standard errors are generally larger at lower wind speeds where the relation between wind and micropressure is less well defined and is subject to changes

in the microbarom level. For the same reason errors near the microbarom peak are also larger. Further discussion of these results, as well as polynomical-based regression results, can be found in Israelsson and McLaughlin (2005).

Prediction Using Statistical Relationship of Micropressure and Wind

As the above discussion makes clear, the relation between wind and micropressure is non-linear – at low wind speeds micropressure variations are less dependent on the wind, while at higher wind speeds the micropressure variations are dominated by wind-induced effects. In other words, the wind-micropressure relation exhibits tail-dependence structure. A weakness of standard regression analysis, as used in the preceding section, is that it cannot cope well with tail-dependence structures. As an alternative, we apply copula theory, a non-linear statistical framework to study non-Gaussian, non-linear dependence structures. Copula theory allows us to form the joint probability distribution of wind and micropressure, from which we can derive non-linear regression curves at any given percentile level. The quantile regression curves could eventually serve as design curves for a constant false alarm rate (CFAR) detector.

A copula is a function that joins or 'couples' a multivariate distribution function to its one-dimensional marginal distribution functions. For a formal framework of copulas see Joe (1997), Nelsen (1999), and Drouet-Mari and Kotz (2001). The basic idea behind the copula formalism is to separate dependence and marginal behavior between elements of multivariate random vectors. For simplicity, we consider bivariate copulas. A great many examples of copulas can be found in the literature and most of the copulas are members of families with one or more real parameters. One important class of copulas is the normal or Gaussian copula. Another important class of copulas is the Archimedean copulas. We discuss the various copulas in much greater detail in Bondár (2005), and confine our discussion here to the use of the Gumbel copula, in the Archimedean class. Note that the Gumbel copula is also an extreme value copula, and exhibits positive upper tail dependence.

We have determined the 50% and 95% quantile regression for the micropressure channel at I08H1 versus a variety of wind, or wind derived quantities, including wind speed, longitudinal wind speed, mean wind speed, and the Bernoulli trace. We generate the 'Bernoulli' trace from the average wind speed and the radial (longitudinal) wind component as $w_{avg} * (w_r - w_{avg})$. This formula follows from Bernoulli's principle, which states that for a laminar flow, small variations in air pressure are proportional to the full derivative of wind speed: $dp \sim w*dw$ where dw denotes the wind fluctuation. While Bernoulli's principle ignores turbulence, it might still serve as a good approximation for the micropressure variations.

In our regressions we used data for each day in the data set shown in Figure 3 and considered a range of copulas. Using the Gumbel copula we obtain good quantile regression fits to the micropressure and Bernoulli data, so we limit the following discussion to these particular results. Furthermore, to facilitate the copula formalism, we work with the envelopes of the various traces.

Figure 10 shows the corresponding quantile regression curves obtained from the Gumbel copula and the micropressure and Bernoulli trace data. The value of copula parameter α and the misfit between the empirical and theoretical K(t) distributions are given in the legends. In some cases (e.g. May 7) the copula fitting procedure suggested that micropressure variations are independent from the wind. This is most likely related to data problems due to the inertia of anemometers at low wind speeds (calms), and to the insufficient sampling of the distribution tails. In order to measure tail dependence, the data set should be large enough to provide a representative sample from the tails of the

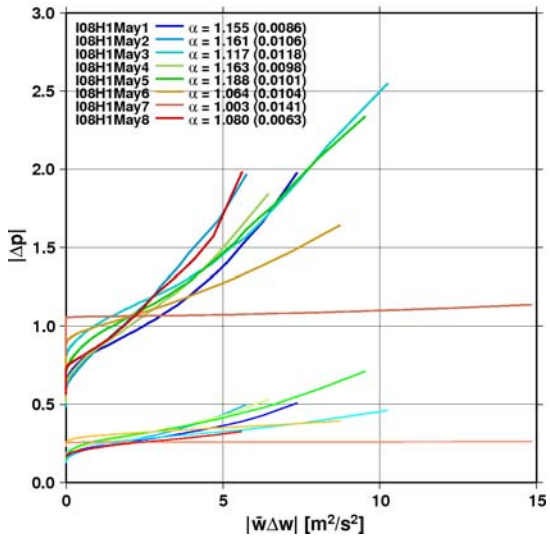

Figure 10. Median and 95% quantile regression curves (lower and upper curves, respectively) of absolute micropressure variations subject to Bernoulli trace at I08BO between May 1 and 8, 2005 derived from the Gumbel copula.

marginal distributions. Furthermore, true signals may contribute to the tails; hence the data set used to derive the regression curves subject to wind should avoid periods with infrasonic signals.

We used the quantile regression curves obtained for I08BO on May 1, 2005 to predict absolute micropressure variations for the rest of the days. Figure 11 shows the absolute micropressure and the Bernoulli traces for May 1, 2005. The green lines in Figure 11 are detections reported by the International Data Centre (IDC), based on use of the Progressive Multi-Channel Correlation (PMCC) algorithm (Cansi, 1995). Unlabeled PMCC detections indicate noise detections. This day should be suitable dfor deriving regression curves, since PMCC made only two signal detections (labeled green lines) on this day.

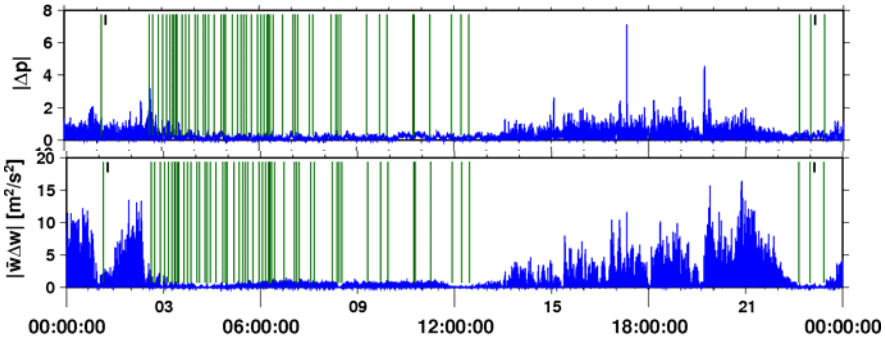

Figure 11. Absolute micropressure (top) and Bernoulli traces (bottom) at I08H1 on May 1, 2005. Green lines denote PMCC detections; unlabeled detections are noise detections.

Figure 12 shows the absolute micropressure variations and the predictions, based on the Bernoulli trace, for May 2-8, 2005 at I08H1, predicted from the corresponding Gumbel quantile regression curves from May 1, 2005. Note that the 95% quantile regression is interpreted such that 95% of the times the absolute micropressure variation is below the 95% quantile regression. If the micropressure variation exceeds this threshold, then it is not explained by the wind.

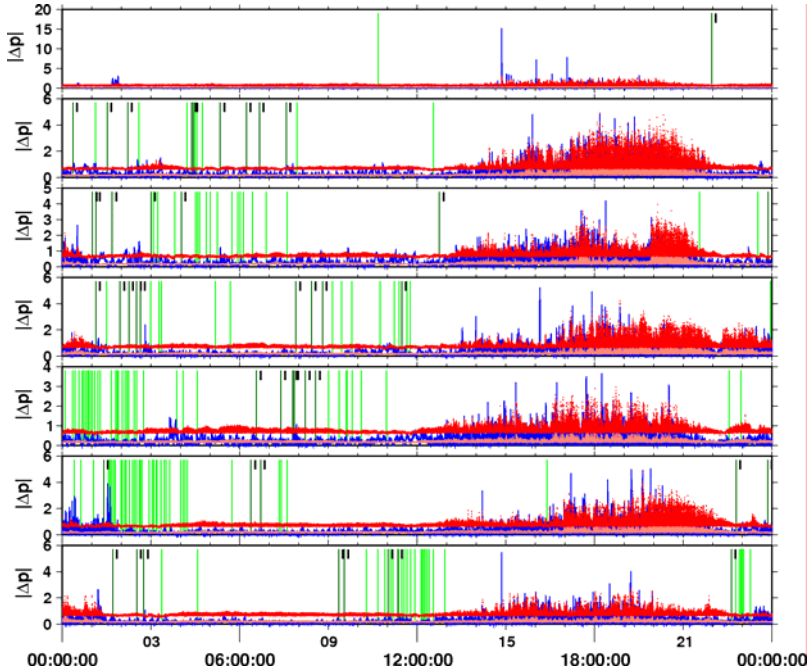

Figure 12. Absolute micropressure (blue) at I08H1 for May 2 to 8, 2005 (bottom to top), with predictions from the Gumbel median (light red) and 95% (dark red) quantile regressions. Regressions based on the micropressure and Bernoulli traces on May 1, 2005. Green lines indicate PMCC detections reported by the IDC.

We are only able to characterize the low frequency micropressure versus wind relations due to the low sample rates used for the wind sensors at IMS stations. Thus, during calm periods, although for most cases the micropressure variations appear to be explained by the wind, the coherence across the array may be carried in higher frequency bands, allowing PMCC to make detections. Similarly, the peaks above the 95% quantile curves could indicate data

problems and may not be coherent in the whole infrasonic frequency band. Nevertheless, there are instances when the micropressure fluctuations persistently exceed the 95% quantile curves without producing PMCC detections. These may indicate missed signals. A more comprehensive discussion of these results, as well as our overall application of a statistical approach to predicting micropressure variations from wind observations, can be found in Bondár (2005).

CONCLUSIONS AND RECOMMENDATIONS

In this study we focused on developing and validating the methodology to characterize the relations between wind and micropressure. We have demonstrated the practical value of wind measurements for understanding the structure of infrasonic noise.

We applied a common methodology to estimate the ambient infrasound noise. This investigation took advantage of the availability of infrasound data on the rapid-access RDSS data archive. These analyses indicate that the median noise amplitude at a given station and frequency may vary by two orders of magnitude depending on time of day or season and may vary among the stations by a factor of about 15 at 0.2 Hz and about 40 at 1 Hz. Ambient noise clearly increases with horizontal wind speed, particularly above a threshold wind speed (which varies among stations). To ensure that the full range of inter-station variability in the noise-wind relationship is captured we recommend that ambient noise at new stations be estimated as data become available. Further, all of the results described here are critically dependent on accurate station parametric (e.g. amplitude and phase response) and environmental (e.g. vegetation at site) metadata. We recommend continued efforts to compile and maintain these metadata.

We found that the overall dependence of micropressure on the mean wind speed is similar for all frequencies and mean wind speeds. At low wind speeds, less than about 1 m/s, there is only a moderate increase in micropressure as the wind speed increases. At high wind speeds, above 2 m/s or so, the micropressure increases rapidly with increasing wind speed. For wind speeds above about 2 m/s the effect of the wind on the micropressure is much larger than that of microbaroms at the stations studied here.

The close correlation between micropressure power spectra and wind speed motivated experiments to predict micropressure amplitudes in the time domain from the mean wind speed. Such predictions can serve to assess the probability that high amplitude micropressure signals are generated by wind gusts or by other sources. We presented two methods for making predictions based on independent estimates of micropressure and wind speed relations. In the first method, we used locally robust regression to model the relationship of mean speed to micropressure based on data from a two week period. We then applied this relationship to data during the subsequent two weeks. The micropressure predictions based on the regression estimates gave similar results for micropressure during wind speeds above 1.5 m/s, with standard errors of less than 3dB for RMS amplitudes in six frequency bands covering frequencies between 0.05 – 4 Hz.

In our second method for making estimates of micropressure from wind speed observations we used a statistical methodology, based on copula theory. We found that the dependence structure of micropressure variations is best described by the Gumbel copula that belongs to the family of Archimedean copulas. The tail-dependence structure described by the Gumbel copula fits the observations well. That is, infrasonic noise becomes dominated by local winds when wind speeds exceed a threshold level. The copula formalism allows us to construct the conditional probability distribution of absolute micropressure subject to wind statistics, and derive quantile regression curves at any given percentile level. The quantile regression curves can serve as design curves for a constant false alarm rate detector, as well as quantify the probability of a detection being a real signal.

In order to derive a robust estimate of the quantile regression curves, the data set must be large enough, preferably void of true signals, to provide sufficient sampling of the tails of the marginal distributions. Our experience shows that at least one day of data is required to get reasonable estimates. The quantile regression curves can then be used to predict micropressure fluctuations for other periods. We found that among the wind statistics we investigated (horizontal wind speed, longitudinal wind speed, average wind speed and Bernoulli trace) the Bernoulli trace offers the most conservative predictions.

The promising results for predicting micropressure from wind speed, as reported here, should be pursued further. For example, we can take azimuth and temporal variations into account, and consider refinements of the regression and statistical models. Issues to consider include investigating the coherence structure of the wind field propagating across the array, investigating the pressure-wind dependence structure at frequencies above 1 Hz, and considering the longitudinal/transverse component of the wind. The systematic application of the regression and copula methodologies to all IMS infrasound stations was beyond the scope of this work. A more comprehensive analysis will be particularly enlightening, given that the IMS infrasound stations are deployed in widely varying environments, with different types of spatial filters.

REFERENCES

Bondár, I. (2005). Statistical Analysis of Wind-generated Infrasound Noise, SAIC Technical Report, in preparation.

Bowman, J.R. (2005a). Meteorological Conditions at Infrasound Stations, *Inframatics,* 9.

Bowman, J.R. (2005b). Meteorological Conditions at Infrasound Stations, SAIC Technical Report SAIC-05/3000.

Bowman, J.R., G.E. Baker, and M. Bahavar (2004a). Infrasound Station Ambient Noise Estimates, SAIC Technical Report SAIC-04/3003.

Bowman, J.R., G.E. Baker, and M. Bahavar (2004b). Infrasound Station Ambient Noise Estimates, Proceedings of the 26th Annual Seismic Research Review, Orlando, FL, 608-617.

Bowman, J. R., G. E. Baker, and M. Bahavar (2005a). Ambient Infrasound Noise, *Geophys. Res. Lett.*, *32*, L09803, doi:10.1029/2005GL022486.

Bowman, J.R., G. Shields, G.E. Baker, and M. Bahavar (2005b). Infrasound Station Ambient Noise Estimates and Models, SAIC Technical Report SAIC-05/3001.

Cansi, Y. (1995). An Automatic Seismic Event Processing for Detection and Location: The PMCC Method, *Geophys. Res. Lett.*, **22**, 1021-1024.

Coyne, J. and I. Henson (1995). Geotool Sourcebook: User's Manual, Teledyne Brown Engineering, Scientific report. no. 1, 01.

Drouet-Mari, D. and S. Kotz (2001). *Correlation and Dependence*, Imperial College Press, London.

Israelsson, H. and K. McLaughlin (2005). Empirical Prediction of Wind Generated Noise at Infrasound Stations, SAIC Technical Report, in preparation.

Joe, H. (1997). *Multivariate Models and Dependence Concepts*, Chapman and Hall, London.

Nelsen, R.B. (1999). *An Introduction to Copulas*, Lecture Notes in Statistics **139**, Springer Verlag, New York.

Shields, F. D. (2005). Low-frequency Wind Noise Correlation in Microphone Arrays, *J. Acoust. Soc. Am.*, 117: 3489-3496.